

Designing Capacitively Coupled Microelectromechanical Filters

Ari T. Alastalo and Ville Kaajakari

Abstract—A design procedure for microelectromechanical band-pass filters is formulated that takes into account specifications set for intermodulation distortion and insertion loss. An integrated receiver architecture, where impedances other than 50 Ω can be used, is found more feasible than resistively terminating the filter at source and load since, for example, a capacitive load makes voltage gain attainable.

I. INTRODUCTION

High-quality-factor resonators are ubiquitous in today's communication devices. Macroscopic ceramic, SAW or FBAR filters offer excellent performance but their large size, high cost and unsuitability for IC integration limit their scope of application. In order to reduce the number of these bulky off-chip filters, receiver architectures such as direct conversion have been developed. However, high-Q filters remain needed as band-select and channel-select filters.

Miniature mechanical resonators, fabricated with microelectromechanical-systems (MEMS) technology, are a potential replacement of off-chip filters as they are compact in size and integratable with IC electronics. The demonstrated quality factors of MEMS resonators, $Q > 100\,000$ at 10 MHz [1] and $Q > 1\,000$ at 1 GHz [2], are comparable to their macroscopic counterparts. While the mechanical properties of MEMS resonators are very promising, the electrostatically coupled resonators characteristically suffer from low electromechanical coupling that leads to high electrical impedance levels and high insertion loss. In order to obtain lower impedances, very narrow gaps are required leading to nonlinear effects due to the inverse capacitance-displacement relationship.

In filter applications, signal intermodulation (IM) due to odd-order nonlinearities is especially detrimental as it can lead to unwanted frequency components within the filter passband. For example, cubic mixing of two fundamental signals having frequencies ω_1 and ω_2 results in third-order intermodulation (IM3) products at frequencies $2\omega_1 - \omega_2$ and $2\omega_2 - \omega_1$. If $\omega_1 = \omega_0 + \Delta\omega$ and $\omega_2 = \omega_0 + 2\Delta\omega$, the IM product at $2\omega_1 - \omega_2$ is at the passband center frequency ω_0 corrupting the desired signal.

In this paper, our prior analysis of in-band [3] and out-of-band [4] filter distortion is summarized and a design procedure for MEMS band-pass filters is formulated that, in addition to insertion loss, takes intermodulation distortion into account. Central challenges for MEMS in high-frequency filter design are identified. Band-pass MEMS filters are shown to be more suitable for novel integrated receiver architectures than for resistive 50- Ω termination at input and output. In particular, an architecture, where the filter is connected directly to an

This work is supported by the Academy of Finland (grant 20542), Aplac Solutions, VTI Technologies, Okmetic, and Tekes (National Technology Agency of Finland). Authors are with VTT Technical Research Center of Finland, VTT Information Technology, Microsensing, Tietotie 3, Espoo, FIN-02044 VTT, Finland (emails: ari.alastalo@vtt.fi, ville.kaajakari@vtt.fi)

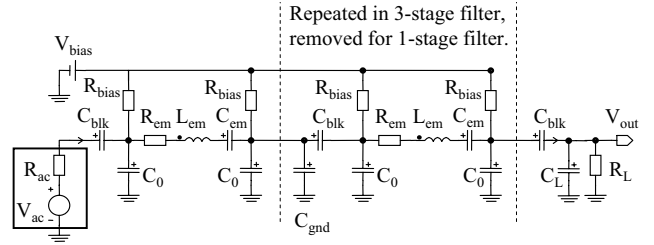


Fig. 1. Schematic for filters made of up to three MEMS resonators. Coupling of the filter stages is done with a shunt capacitance C_{gnd} . The DC-blocking capacitance is denoted C_{blk} .

antenna and to LNA at input and output, respectively, is considered. The design procedure is exemplified for GSM 900.

II. THEORY OF INTERMODULATION IN MEMS FILTERS

Electrical equivalent model for one-, two- and three-stage MEMS filters is shown in Fig. 1 with the inter-stage coupling done with a shunt capacitance C_{gnd} [5]. Here $R_{\text{em}} = \gamma/\eta^2$, $L_{\text{em}} = m/\eta^2$ and $C_{\text{em}} = \eta^2/k$ are the RLC-equivalent parameters of the MEMS resonator with spring coefficient k , effective mass m , resonance frequency $\omega_{\text{res}} = \sqrt{k/m}$ and dissipation $\gamma = \sqrt{km}/Q$. The electromechanical coupling coefficient is $\eta = C_0 V_{\text{bias}}/d$, where C_0 is the rest capacitance of the electrostatic transducers, V_{bias} is the bias voltage, and d is the transducer gap. For the single-resonator filter, the loaded in-circuit quality factor Q' can be calculated as

$$Q' = \sqrt{k'm}/\gamma'. \quad (1)$$

Here

$$\gamma' = \eta^2 (R_{\text{em}} + R'_S + R'_L) \quad (2)$$

$$k' = \eta^2 (1/C_{\text{em}} + 1/C'_S + 1/C'_L) - 2k_e, \quad (3)$$

where R'_S , C'_S , R'_L and C'_L are the series-equivalent resistances and capacitances of the parallel source ($R_{\text{ac}}||C_0$) and load ($R_L||C_0$) circuits, respectively

$$R'_S = \frac{R_{\text{ac}}}{(R_{\text{ac}}\omega C_0)^2 + 1} \quad (4)$$

$$C'_S = \frac{C_0 [(R_{\text{ac}}\omega C_0)^2 + 1]}{(R_{\text{ac}}\omega C_0)^2} \quad (5)$$

$$R'_L = \frac{R_L}{[R_L\omega(C_0 + C_L)]^2 + 1} \quad (6)$$

$$C'_L = \frac{(C_0 + C_L) \{ [R_L\omega(C_0 + C_L)]^2 + 1 \}}{[R_L\omega(C_0 + C_L)]^2}, \quad (7)$$

and $k_e \equiv \eta V_{\text{bias}}/d$ is the electromechanical spring coefficient. In addition to using the loaded Q value of (1), the Thévenin-equivalent input voltage

$$V'_{\text{ac}} = V_{\text{ac}} \frac{1}{1 + j\omega C_0 R_{\text{ac}}} \quad (8)$$

must be used in order to utilize the unloaded IIP3 and SIR results of [3] and [4] for tightly-coupled filters as in what follows.

Signal-to-intermodulation ratio (SIR) in the output of a capacitively-coupled MEMS single-resonator filter for interferers outside the passband is given in [4]. For present purposes, we assume that the pass-band desired-signal frequency $\omega_0 = \omega' \equiv \sqrt{k'/m}$ is much higher than the frequency separation $\Delta\omega$ to the interferers present at the filter input at frequencies $\omega_1 = \omega_0 + \Delta\omega$ and $\omega_2 = \omega_0 + 2\Delta\omega$ and that the bias voltage is much lower than the electromechanical pull-in voltage at which bias level the resonator becomes unstable. With these assumptions, Eq. (23) of [4] simplifies as

$$\text{SIR} = \frac{8|\Delta\omega|\omega_0 V_{\text{bias}}^2 \sqrt{P_{\text{sig}}}}{5\omega_e^2 R'_S P_{\text{int}} \sqrt{P_{\text{int}}}}, \quad (9)$$

where $\omega_e \equiv \sqrt{k_e/m}$. The AC-source powers (see Fig. 1) for the signal and interference are $P_{\text{sig}} = V_{\text{ac,sig}}^2/(2R_{\text{ac}})$ and $P_{\text{int}} = V_{\text{ac,int}}^2/(2R_{\text{ac}})$, respectively. The AC power corresponding to the third-order input intercept point (IIP3) is related to SIR as

$$P_{\text{IIP}} = \text{SIR} \sqrt{\frac{P_{\text{int}}^3}{P_{\text{sig}}}}. \quad (10)$$

When the interferers are inside the passband, we have [3]

$$P_{\text{IIP}}^{\text{IB}} = \frac{V_{\text{bias}}^2}{R'_S \sqrt{(6q^3 + q/2)^2 + 9q^4}}, \quad (11)$$

where $q = Q' \omega_e^2/\omega'^2 = Q' k_e/k'$.

As an example, we consider the one-, two- and three-stage filters of Fig. 1 with the 13-MHz bulk-acoustic-wave (BAW) MEMS resonators of [4] with $Q = 47000$ but with a reduced gap of 25.5 nm in order to have a low mechanical impedance of 38 Ω . We use $C_{\text{gnd}} = 20$ pF and $C_{\text{gnd}} = 30$ pF for the two-stage and three-stage filters, respectively. Furthermore, we set $C_L = 0$ and $R_L = R_{\text{ac}}$ in Fig. 1. Figure 2 shows simulated responses of the filters with 2 Ω (unloaded, $R_{\text{ac}} \ll R_{\text{em}}$) and 450 Ω (loaded, $R_{\text{ac}} \gg R_{\text{em}}$) source and load impedances. The 450 Ω source and load yields $Q' = 1900$ for the in-circuit quality factor (1) of the resonator. Figure 3 shows the analytic and simulated IIP3 input voltage for the filters with ω_0 as shown in Fig. 2. The analytic result, calculated with the exact formulas of [4], approaches (9) and (10) (marked as approximation in Fig. 3) as $\Delta\omega \rightarrow \infty$ and (11) as $\Delta\omega \rightarrow 0$. Equations (9) and (10) become valid as the results for $\Delta f > 0$ and $\Delta f < 0$ approach each other at high frequencies. It is seen that, as expected in [4], outside the passband the unloaded single-resonator result is also valid for the higher-order filters as well as for the tightly-coupled filters.

As another example, we consider 1 GHz single-stage filters based on the resonators of [2] with $k = 373.1$ MN/m, $f_{\text{res}} = 1.150$ GHz and $Q = 5100$. The load of the filter is thought to be a FET amplifier stage with $R_L = 1$ M Ω and $C_L = 1$ pF in Fig. 1. This does not reduce the in-circuit Q value in (1) as much as resistive termination at both sides of the filter. Furthermore, by effectively tapping the mechanical RLC resonator, voltage gain becomes attainable enabling the use of resonators with $R_{\text{em}} \sim 1$ k Ω without introducing significant signal attenuation. The filter is thought to be directly connected to an antenna, where different impedances can be realized

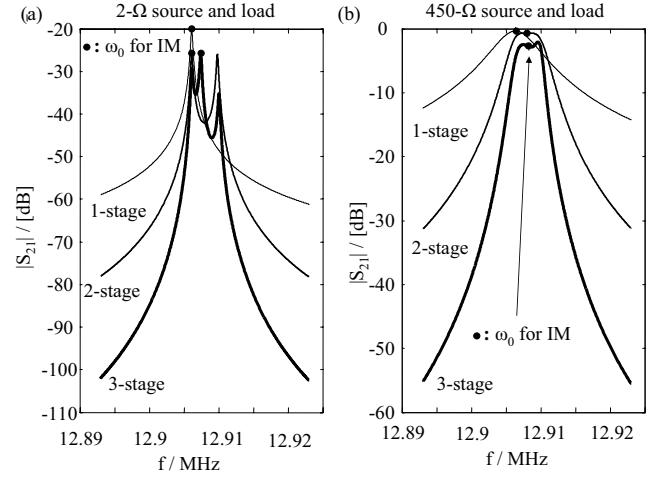


Fig. 2. Unloaded (a) and loaded (b) response of the filters composed of one, two and three BAW resonators of [4] as shown in Fig. 1.

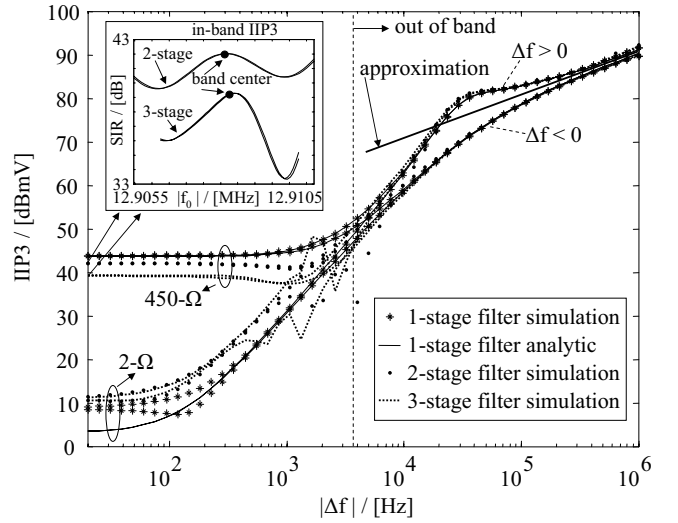


Fig. 3. Input voltage corresponding to IIP3 as function of the interferer frequency separation $\Delta f = 2\pi\Delta\omega$ for the filters of Fig. 2 with a -20 dBmV desired signal at ω_0 and with 0 dBmV interferers. The inset at the upper left corner shows the in-band IIP3 for the loaded two-stage and three-stage filters with $\Delta f = 20$ Hz and with the signal frequency f_0 swept across the passband.

but the different impedance levels can also be realized with a transformer. For given impedance level, the source voltage V_{ac} is calculated from source power level.

Table I shows relevant parameters for three different filter configurations where (A) is based on the resonator of [2] while for (B) and (C) the mechanical impedance is reduced to $R_{\text{em}} \approx 50$ Ω by changing the bias voltage and the gap. The pass-band voltage gain is

$$G_V = 20 \log_{10} \frac{V_{\text{out}}(f')}{V_{\text{ac}}/2}, \quad (12)$$

where V_{ac} and V_{out} are as shown in Fig. 1.

Table II shows the resulting SIR, when the filters (A), (B) and (C) of Table I are used as a front-end filter for GSM 900. The signal and interference powers are as specified in [6]. It is seen that two 0-dBm interferers at 10 MHz and 20 MHz separation from the desired signal reduce the SIR below

TABLE I

PARAMETERS FOR THE FILTER CONFIGURATIONS. (A) THE THEORETICAL RESONATOR OF [2]. (B) SAME AS A BUT SCALED TO $R_{EM} \approx 50 \Omega$ BY INCREASING THE BIAS VOLTAGE. (C) SAME AS A BUT SCALED TO $R_{EM} \approx 50 \Omega$ BY REDUCING THE GAP.

	A	B	C	
V_{bias}	40	147	16	V
d	30	30	10	nm
ω_e	152	560	316	10^6 rad/s
R_{ac}	1000	50	50	Ω
R'_S	690	49.9	49.5	Ω
R_{em}	663	49	51	Ω
C_0	93	93	278	fF
Q'	2500	2500	2600	
f'	1.149	1.143	1.148	GHz
G_V	-16	8.3	6.7	dB

TABLE II

SIR FOR THE RESONATORS OF TABLE I USED AS A FILTER FOR GSM 900. THE SIGNAL POWER IS $P_{sig} = -99$ DBM. THE INTERFERER POWERS ARE AS SPECIFIED IN [6].

GSM 900		resulting SIR		
Δf	P_{int}	A	B	C
-10	0	-2	14	-10
-3	-23	55	63	44
-0.6	-43	96	87	76
0.6	-43	111	90	85
3	-23	59	77	58
10	0	-1	28	-5
MHz	dBm	dB	dB	dB

acceptable levels except for filter (B) for which the bias voltage is not feasible at least in portable devices.

III. FILTER DESIGN

In what follows, we aim to design a single-stage MEMS front-end filter for $f_0 = 1$ GHz with requirements of GSM 900 mobile device. We consider the architecture, where the filter input is connected directly to an antenna and at the filter output we have a capacitive FET LNA stage with $C_L = 1$ pF in Fig. 1 (R_L high enough to be ignored $\Rightarrow R'_L = 0$ and $C'_L = C_L + C_0$ in (6) and (7), respectively).

Let us first estimate the required in-circuit Q value in (1) for a single-stage filter. Minimum attenuation requirement for the filter, to be as good as the minimum-performance band-select filters, is that the out-of-GSM-RX-band interferers are suppressed to the same level as the strongest in-band interferers. Thus the filter has to have $A_{min} \equiv 23$ dB more attenuation at 10 MHz off the passband than at the passband [6]. If this is achieved, the linearity requirement for the LNA is set by the in-band interferers that normally are not affected by band-select filtering. For the single-stage MEMS filter, we thus find

$$Q' \geq \frac{\sqrt{A_{min}^2 - (f/f_0)^2}}{|1 - (f/f_0)^2|} \equiv Q'_{min} \approx 700. \quad (13)$$

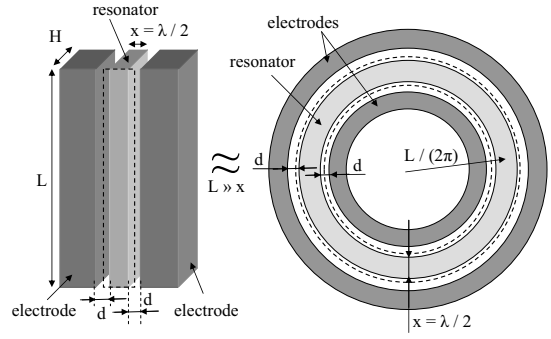


Fig. 4. Test geometry for resonator design showing the resonator surrounded by the electrodes. The dotted line indicates the vibration mode shape in extended state.

For channel-select filtering, the passband is 200 kHz, which would need a much higher in-circuit Q factor of $Q' = 1$ GHz / 200 kHz = 5000. A Q value of $Q' = 5000$ would also be enough for $A_{min} = 40$ dB at 10 MHz off the passband in (13), which typically is the case for commercial FBAR filters. Increasing the filter order makes the stop-band response a steeper function of frequency and thus a lower quality factor for the resonators becomes sufficient.

For the pass-band voltage gain (12), we require $G_V(f_0) \geq G_{min} \equiv -3$ dB. For the single-stage filter of Fig. 1, this leads to

$$R_{em} \leq \frac{2}{\omega_0 (C_0 + C_L) G_{min} |1 + j\omega_0 C_0 R_{ac}|} R'_S \equiv R_{em}^{max}. \quad (14)$$

For higher-order filters, an approximation for the maximum mechanical resistance can be obtained by dividing the single-stage result (14) by the filter order.

As the out-of-GSM-RX-band interferers with $\Delta f = 10$ MHz were found the most detrimental in Table II, we require $SIR \geq SIR_{min} = 9$ dB (full-rate speech [6]) at the output of the filter when in the filter input we have a desired signal at f_0 with $P_{sig} = -99$ dBm and two interferers at $f_0 + 10$ MHz and $f_0 + 20$ MHz with $P_{int} = 0$ dBm [6]. Consequently, (9) yields:

$$\frac{\omega_e^2 R'_S}{V_{bias}^2} = \frac{C_0 R'_S}{md^2} \leq \frac{7 \times 10^{15}}{SIR_{min}} \frac{1}{Ws^2} \equiv W_e^{max}, \quad (15)$$

which is also valid for higher-order filters as shown in Sec. II.

Considering signal self distortion with $P_{int} = P_{sig} = P_{sig}^{max} = -38$ dBm [6], (10) gives for the required minimum in-band IIP3 a value of -33.5 dBm. On the other hand, considering an in-band interference with $P_{int} = -49$ dBm [6] and a signal with $P_{sig} = -99$ dBm, (10) gives a more demanding requirement of

$$P_{IIP}^{IB} \geq -19.5 \text{ dBm} \equiv P_{IIP,min}^{IB}, \quad (16)$$

where P_{IIP}^{IB} is given by (11). As discussed in Sec. II, for higher-order filters, the in-band IIP3 depends on the desired-signal frequency within the passband.

Let us now, as a simple example, consider a bar geometry shown in Fig. 4. The resonating dimension is $x = \lambda/2 = v/(2f_0) \approx 4 \mu\text{m}$ for $f_0 = 1$ GHz. Here $v = \sqrt{Y/\rho}$ is the bulk-acoustic wave velocity with $\rho = 2330$ kg/m³ the density and $Y = 168$ GPa the Young's modulus of silicon. This simple geometry can also approximate the ring geometry

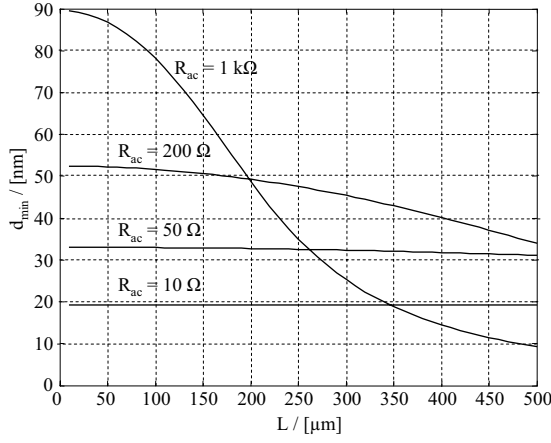


Fig. 5. Minimum gap (19), determined by the maximum out-of-band intermodulation, for the resonators of Fig. 4 with $H = 10 \mu\text{m}$.

[7], shown at the right-hand side of Fig. 4, when the ring radius $L/(2\pi)$ is much larger than the ring thickness x . The capacitive transducers at both sides of the resonator have an area of $A = HL$ and rest capacitance of $C_0 = \epsilon_0 HL/d$, where d is the gap. The effective mass and spring coefficient are now [8]

$$m = \rho LxH/2 \quad (17)$$

$$k = \pi^2 YLH/(2x). \quad (18)$$

Equation (15) now leads to a requirement for the minimum gap

$$(R_{ac}\omega_0\epsilon_0LH)^2 d + d^3 \geq \frac{4\epsilon_0 R_{ac}}{\rho\lambda W_e^{\max}} \quad (19)$$

that is easily evaluated numerically. Figure 4 shows the minimum gap for $R_{ac} \in \{10, 50, 200, 1000\} \Omega$ as a function of the transducer length L with $H = 10 \mu\text{m}$. If $R'_S \approx R_{ac} \Leftrightarrow (R_{ac}\omega_0 C_0)^2 \ll 1$, we find

$$d \geq d_{\min} = \left(\frac{4\epsilon_0 R_{ac}}{\rho\lambda W_e^{\max}} \right)^{1/3}, \quad (20)$$

that gives, for example, $d_{\min} = 19 \text{ nm}$ and $d_{\min} = 33 \text{ nm}$ for $R_{ac} = 10 \Omega$ and $R_{ac} = 50 \Omega$, respectively, as in Fig. 5. The increase in minimum gap d_{\min} with increasing source impedance R_{ac} is due to increasing voltage levels at higher impedances.

We now set the gap close to its minimum value for the resonators of Fig. 5, say $d = d_{\min} + 3 \text{ nm}$, after which C_0 and R'_S are determined and the maximum electromechanical resistance can be calculated from (14) and used to find the minimum value for QV_{bias}^2 since $R_{\text{em}} = d^2 \sqrt{km} / (QC_0^2 V_{\text{bias}}^2)$, namely

$$QV_{\text{bias}}^2 \geq \frac{d^2 \sqrt{km}}{C_0^2 R_{\text{em}}^{\max}} \equiv (QV^2)_{\min}. \quad (21)$$

Figure 6 now illustrates one of the central challenges in MEMS filter design for portable low-voltage devices, namely, QV_{bias}^2 has to be very high. For example, assuming $Q = 10000$ and $V = 10 \text{ V}$, requirement (21) can be met for $R_{ac} = 50 \Omega$ with $L = 300 \mu\text{m}$ (a), which is a very large resonator. If $R_{ac} = 10 \Omega$ and $V_{\text{bias}} = 6 \text{ V}$, a smaller resonator of $L = 100 \mu\text{m}$ with $Q = 10000$ (b) or $L = 200 \mu\text{m}$ with $Q = 6000$ (c) is enough.

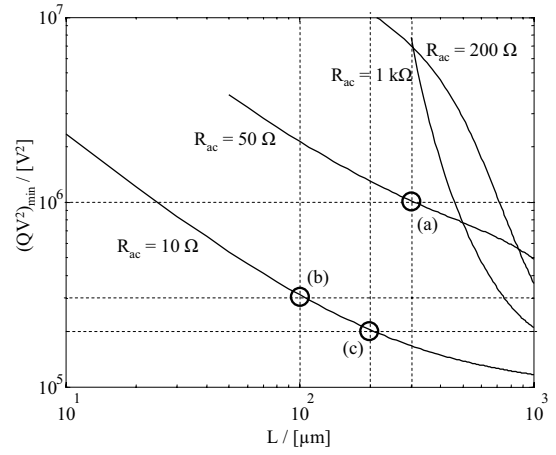


Fig. 6. Minimum of QV_{bias}^2 (21), determined by the maximum in-band loss of the filter, corresponding to the resonator geometries of Fig. 5 with $d = d_{\min} + 3 \text{ nm}$.

We now consider the case (c) of Fig. 6 with $C_L = 1 \text{ pF}$, $H = 10 \mu\text{m}$, $L = 200 \mu\text{m}$, $R_{ac} = 10 \Omega$, $d = 22 \text{ nm}$, $V_{\text{bias}} = 6 \text{ V}$ and $Q = 6000$ resulting in $C_0 = 800 \text{ fF}$, $R'_S = 9.97 \Omega$, $C'_S = 316 \text{ pF}$, $m = 9.9 \text{ pkg}$, $k = 391 \text{ MN/m}$, $C'_{\text{em}} = 123 \text{ aF}$, $L_{\text{em}} = 0.2 \text{ mH}$, $R_{\text{em}} = 215 \Omega$, $\omega_e = 78 \times 10^6 \text{ rad/s}$, $R_{\text{em}}^{\max} = 239 \Omega > R_{\text{em}}$, $\text{SIR} = 12.5 \text{ dB} > \text{SIR}_{\min}$, $Q' = 5700 > Q'_{\min}$, $q = 0.88$, $P_{\text{IP}}^{\text{IB}} = 28.5 \text{ dBm} > P_{\text{IP},\min}^{\text{IB}}$ and $U_{\text{pull-in}} = 343 \text{ V} \gg V_{\text{bias}}$.

Lowering the load capacitance, gives somewhat more design freedom and one finds a solution with $C_L = 0.1 \text{ pF}$, $H = 10 \mu\text{m}$, $L = 100 \mu\text{m}$, $R_{ac} = 10 \Omega$, $d = 22 \text{ nm}$, $V_{\text{bias}} = 5 \text{ V}$ and $Q = 5000$ resulting in $R_{\text{em}} = 743 \Omega$, $R_{\text{em}}^{\max} = 884 \Omega$, $\text{SIR} = 12.5 \text{ dB}$ and $P_{\text{IP}}^{\text{IB}} = 32.5 \text{ dBm}$.

For resistive load ($R_L = R_{ac}$ and $C_L \rightarrow 0$) R_{em}^{\max} is reduced below R_{ac} and the minimum of QV_{bias}^2 is significantly increased.

IV. CONCLUSION

A procedure to design MEMS band-pass filters, with specifications set for maximum in-band loss and intermodulation distortion, is formulated. Limitations obtained for the transducer gap, bias voltage and resonator quality factor illustrate the challenges for MEMS to be feasible in high-frequency filters. It is found desirable to utilize the high resonator quality factor for voltage gain that is enabled by capacitive load termination at the output of the filter.

REFERENCES

- [1] V. Kaajakari et al., *IEEE Electron Device Lett.*, vol. 25, no. 4, pp. 173–175, Apr. 2004.
- [2] J. Wang, Z. Ren, and C. T.-C. Nguyen, *IEEE Trans. Ultrason., Ferroelect., Freq. Contr.*, vol. 51, no. 12, pp. 1607–1628, Dec. 2004.
- [3] A. T. Alastalo and V. Kaajakari, *IEEE Electron Device Lett.*, vol. 26, no. 5, pp. 289–291, May 2005.
- [4] A. T. Alastalo and V. Kaajakari, *IEEE Journal of Microelectromechanical Systems*, accepted, 2005.
- [5] Siavash Pourkamali and Farrokh Ayazi, *Sensors and Actuators A, Physical*, vol. 122, no. 2, pp. 307–316, Aug 2005.
- [6] ETSI, “GSM Global System for Mobile Communications, 3GPP TS 05.01, 05.05 and 05.08,” 1999.
- [7] Sheng-Shian Li, Yu-Wei Lin, Yuan Xie, Zeying Ren, and Clark T.-C. Nguyen, *IEEE MEMS'04*, pp. 821–824.
- [8] T. Mattila et al., *Sensors and Actuators A: Physical*, vol. 101, issue 1–2 pp. 1–9, Sep 2002.